

Article

Molecular Structures of the Pyridine-2-olates $\text{PhE}(\text{pyO})_3$ ($E = \text{Si}, \text{Ge}, \text{Sn}$)—[4+3]-Coordination at Si, Ge vs. Heptacoordination at Sn

Sarah Kuß¹, Erica Brendler²  and Jörg Wagler^{1,*} ¹ Institut für Anorganische Chemie, TU Bergakademie Freiberg, D-09596 Freiberg, Germany² Institut für Analytische Chemie, TU Bergakademie Freiberg, D-09596 Freiberg, Germany

* Correspondence: joerg.wagler@chemie.tu-freiberg.de; Tel.: +49-3731-39-4343

Abstract: The phenyltetrel pyridine-2-olates $\text{PhE}(\text{pyO})_3$ ($E = \text{Si}, \text{Ge}, \text{Sn}$; $\text{pyO} = \text{pyridine-2-olate}$) were synthesized from the respective chlorides PhECl_3 and 2-hydroxypyridine (2-pyridone) with the aid of a sacrificial base (triethylamine). Their solid-state structures were determined by single-crystal X-ray diffraction. $\text{PhSi}(\text{pyO})_3$ exhibits a three-fold capped tetrahedral Si coordination sphere ([4+3]-coordination, $\text{Si}\cdots\text{N}$ separations ca. 3.0 Å), in accordance with structures of previously reported silicon pyridine-2-olates. $\text{PhGe}(\text{pyO})_3$ adopts a related [4+3]-coordination mode, which differs in terms of the tetrahedral faces capped by the pyridine N atoms. Additionally, shorter $\text{Ge}\cdots\text{N}$ separations (2.8–2.9 Å) indicate a trend toward tetrel hypercoordination. $\text{PhSn}(\text{pyO})_3$ features heptacoordinate tin within a pentagonal bipyramidal Sn coordination sphere ($\text{Sn}\cdots\text{N}$ separations 2.2–2.4 Å). For the Si and Sn compounds, ²⁹Si and ¹¹⁹Sn NMR spectroscopy indicates retention of their tetrel coordination number in chloroform solution.

Keywords: 2-hydroxypyridine; hypercoordination; ¹¹⁹Sn solid-state NMR; tetrel; X-ray diffraction

**Citation:** Kuß, S.; Brendler, E.;Wagler, J. Molecular Structures of the Pyridine-2-olates $\text{PhE}(\text{pyO})_3$ ($E = \text{Si}, \text{Ge}, \text{Sn}$)—[4+3]-Coordination at Si, Ge vs. Heptacoordination at Sn. *Crystals* **2022**, *12*, 1802. <https://doi.org/10.3390/cryst12121802>

Academic Editor: Alexander Y. Nazarenko

Received: 14 November 2022

Accepted: 3 December 2022

Published: 10 December 2022

Publisher's Note: MDPI stays neutral with regard to jurisdictional claims in published maps and institutional affiliations.



Copyright: © 2022 by the authors. Licensee MDPI, Basel, Switzerland. This article is an open access article distributed under the terms and conditions of the Creative Commons Attribution (CC BY) license (<https://creativecommons.org/licenses/by/4.0/>).

1. Introduction

In previous studies [1–3] it was shown that in silicon pyridine-2-olates the potentially bidentate pyO group ($\text{pyO} = \text{pyridine-2-olate}$) is essentially monodentate, bound to Si through an Si–O bond and capping tetrahedral faces of the Si coordination sphere by rather remote $\text{N}\cdots\text{Si}$ coordination (e.g., in compounds **I** [2] and **II** [3], Figure 1). In addition, it has been shown that pyridine-2-olates may serve as bridging ligands with their N atom coordinating to a transition metal (TM) atom, thus fostering the formation of heteronuclear $\text{Si}\cdots\text{TM}$ complexes with higher-coordinate Si atom, for example in compounds **III** and **IV** [2] and some others [2,4]. Whereas in $\text{pyO-TM-silyl-complexes}$ with tetracoordinate Si atom and thus formally covalent TM–Si bond (such as **V** [5] and **VI** [6]) pyO ligand(s) may buttress this diatomic core and thus simply add some stability, in cases with formally dative bonding or weak $\text{TM}\cdots\text{Si}$ attraction the availability of dangling N-donor sites in silicon pyridine-2-olates may be a key toward their binding to transition metals. With the perspective of extending studies of $\text{pyO-bridged TM-tetrel-complexes}$ to heavier congeners of Si, the mode(s) of pyO-coordination at the heavier congeners (Ge, Sn) may hint at their suitability as starting materials for $\text{pyO-bridged tetrel-TM complexes}$. So far, molecular structures (in terms of crystallographically proven configurations) of germanium pyridine-2-olates are unknown [7]. For Sn- pyO-compounds , two crystal structures have been reported for compounds with penta- [8] or penta- and hexacoordinate Sn [9] in which the pyridine-2-olate is bridging two Sn atoms (with Sn–O and Sn–N bonds). These examples, however, involve a distannamethane motif [8] or a combination of different Sn sites (SnBu_2 and SnBu_3 groups) [9]. Crystallographic studies of pyO coordination in rather simple organotin compounds are yet to be performed. In the current study, we present a systematic comparison of the solid-state structures of the series of related phenyltetrel

compounds $\text{PhE}(\text{pyO})_3$ ($E = \text{Si}, \text{Ge}, \text{Sn}$). Whereas our interest in these compounds mainly arises from aspects of coordination chemistry (coordination of bidentate ligands at the tetrel and as bridging ligands between tetrel and transition metal), the exploration of coordination compounds of heavier tetrrels with pyridine bases may also be of interest for other research fields. Both pyridine bases as ligands [10,11] and tin as a central atom [12] are the focus of the development of anti-cancer drugs.

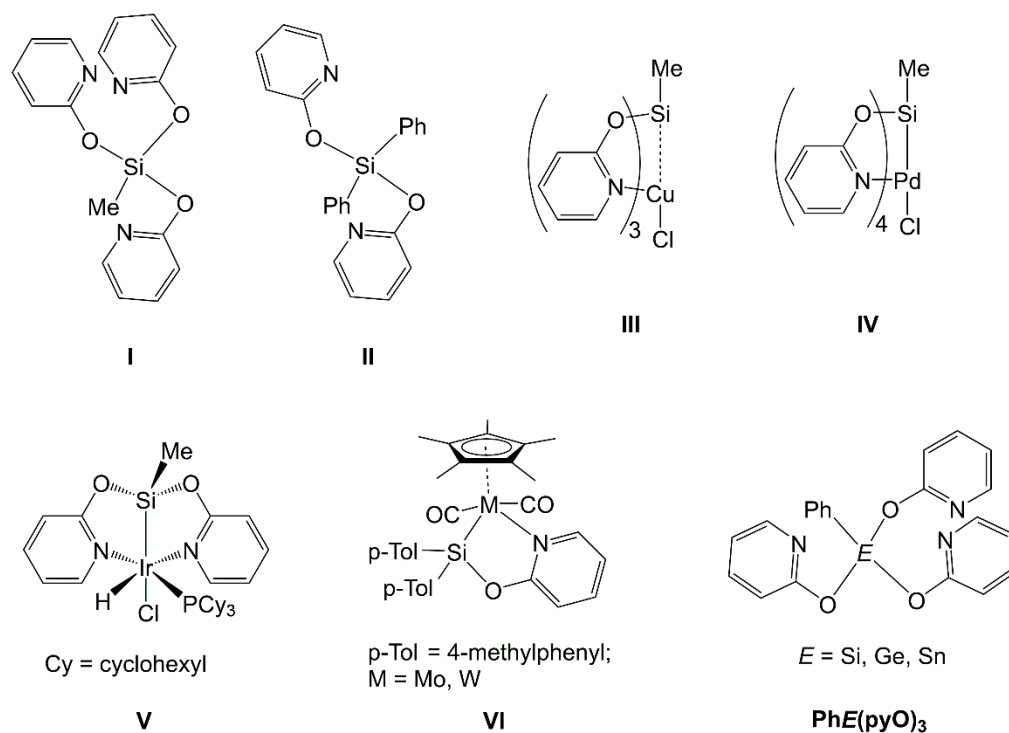


Figure 1. Selected pyridine-2-olate compounds of silicon with remote $\text{N}\cdots\text{Si}$ coordination (I,II), with hypercoordinate Si atom featuring a metal atom in the coordination sphere (III,IV) and with tetracoordinate Si bound to a transition metal atom (V,VI) as well as a generic representation of the compounds ($\text{PhE}(\text{pyO})_3$) under investigation in this paper.

2. Materials and Methods

2.1. General Considerations

Starting materials 2-hydroxypyridine (ABCR, Karlsruhe, Germany, 98%), phenyltrichlorosilane (Wacker, Burghausen, Germany), phenyltrichlorogermane (Gelest, Tullytown, PA, USA, 95%) and phenyltrichlorostannane (Sigma-Aldrich, Steinheim, Germany, 98%) were used as received without further purification. THF, diethyl ether, and triethylamine were distilled from sodium/benzophenone and kept under argon atmosphere. Chloroform, stabilized with amylenes (Honeywell, Seelze, Germany, $\geq 99.5\%$) and CDCl_3 (Deutero, Kastellaun, Germany, 99.8%) were stored over activated molecular sieves (3 \AA) for at least 7 days and used without further purification. All reactions were carried out under an atmosphere of dry argon utilizing standard Schlenk techniques. Solution NMR spectra (^1H , ^{13}C , ^{29}Si , ^{119}Sn) (cf. Figures S1–S9 in the supporting information) were recorded on Bruker Avance III 500 MHz and Bruker Nanobay 400 MHz spectrometers. ^1H , ^{13}C and ^{29}Si chemical shifts are reported relative to Me_4Si (0 ppm) as internal reference. ^{119}Sn chemical shifts are reported relative to Me_4Sn (0 ppm) with external referencing. ^1H and ^{13}C NMR signals were assigned in accord with mutual coupling patterns (in case of ^1H) and according to the shifts of corresponding ^1H or ^{13}C NMR signals in related compounds $\text{MeSi}(\text{pyO})_3$ [2], $\text{Ph}_2\text{Si}(\text{pyO})_2$ [3] and $\text{PhP}(\text{pyO})_2$ [13]. Furthermore, ^1H – ^{13}C HSQC techniques were employed for ^{13}C NMR signal assignment of compound $\text{PhSn}(\text{pyO})_3$. The ^{119}Sn MAS NMR spectrum of $\text{PhSn}(\text{pyO})_3$ was recorded on a Bruker Avance 400 WB spectrometer using a 4 mm zirconia (ZrO_2) rotor and an MAS frequency of $\nu_{\text{spin}} = 13 \text{ kHz}$. The

chemical shift is reported relative to Me_4Sn (0 ppm) and was referenced with the aid of a sample of SnO_2 ($\delta_{\text{iso}} = -603$ ppm). Determination of the chemical shift anisotropy (CSA) tensor principal components from the spinning sideband spectrum was carried out with the SOLA module contained in the Bruker software package TOPSPIN. Principal components δ_{11} , δ_{22} , δ_{33} as well as span Ω and skew κ are reported according to the Herzfeld–Berger notation [14,15]. Elemental analyses were performed on an Elementar Vario MICRO cube. For single-crystal X-ray diffraction analyses, crystals were selected under an inert oil and mounted on a glass capillary (which was coated with silicone grease). Diffraction data were collected on a Stoe IPDS-2/2T diffractometer (STOE, Darmstadt, Germany) using $\text{Mo K}\alpha$ -radiation. Data integration and absorption correction were performed with the STOE software XArea and XShape, respectively. The structures were solved by direct methods using SHELXS-97 or SHELXT and refined with the full-matrix least-squares methods of F^2 against all reflections with SHELXL-2014/7 [16–19]. All non-hydrogen atoms were anisotropically refined, and hydrogen atoms were isotropically refined in idealized position (riding model). For details of data collection and refinement (incl. the use of SQUEEZE in the refinement of the structure of $\text{PhSi}(\text{pyO})_3 \cdot \text{THF}$) see Appendix A, Table A1. Graphics of molecular structures were generated with ORTEP-3 [20,21] and POV-Ray 3.7 [22]. CCDC 2217508 ($\text{PhSi}(\text{pyO})_3 \cdot \text{THF}$), 2217510 ($\text{PhSi}(\text{pyO})_3 \cdot \text{CHCl}_3$), 2217509 ($\text{PhGe}(\text{pyO})_3$), and 2217511 ($\text{PhSn}(\text{pyO})_3$) contain the supplementary crystal data for this article. These data can be obtained free of charge from the Cambridge Crystallographic Data Centre via <https://www.ccdc.cam.ac.uk/structures/> (accessed on 4 November 2022).

2.2. Syntheses and Characterization

Compound $\text{PhSi}(\text{pyO})_3 \cdot \text{THF}$ ($\text{C}_{25}\text{H}_{25}\text{N}_3\text{O}_4\text{Si}$). A Schlenk flask was charged with magnetic stirring bar and 2-hydroxypyridine (2.00 g, 20.8 mmol), then evacuated and set under Ar atmosphere prior to adding THF (70 mL) and triethylamine (2.50 g, 24.7 mmol). The resultant mixture was stirred at room temperature, and phenyltrichlorosilane (1.60 g, 7.56 mmol) was added dropwise via syringe through a septum. Upon completed addition of silane, stirring was continued for 30 min, whereupon the flask was stored at 5 °C overnight. Thereafter, the triethylamine hydrochloride precipitate was removed by filtration and washed with THF (2×5 mL). From the combined filtrate and washings, the solvent was removed under reduced pressure (condensation into a cold trap) to afford a colorless solid. This crude product was dissolved into hot THF (4 mL) and allowed to crystallize upon cooling to room temperature. From this coarse crystalline product (thick colorless needles) of $\text{PhSi}(\text{pyO})_3 \cdot \text{THF}$ the supernatant was removed by decantation; the crystals were washed with THF (2×5 mL) and briefly dried in vacuum. Yield: 2.29 g (4.98 mmol, 66%). The yield is reported with respect to the composition $\text{PhSi}(\text{pyO})_3 \cdot \text{THF}$, which is in accord with the composition of a single crystal taken from the freshly crystallized product for single-crystal X-ray diffraction analysis. ^1H NMR spectroscopy (cf. Figure S1 in the supporting information) already indicates some loss of THF upon drying. This effect was also found with elemental analysis: elemental analysis for $\text{C}_{21}\text{H}_{17}\text{N}_3\text{O}_3\text{Si} \cdot 0.5 \text{ THF}$ ($423.52 \text{ g} \cdot \text{mol}^{-1}$): C, 65.23%; H, 5.00%; N, 9.92%; found C, 65.21%; H, 5.10%; N, 9.96%. ^1H NMR (CDCl_3): δ (ppm) 8.11–8.07 (m, 2H, Ph-o), 8.01 (m, br, 3H, H^6), 7.52 (m, br, 3H, H^4), 7.44–7.32 (m, 3H, Ph-m/p), 6.92 (d, br, 3H, 8.2 Hz, H^3), 6.82 (m, br, 3H, H^5); $^{13}\text{C}\{^1\text{H}\}$ NMR (CDCl_3): δ (ppm) 160.3 (C^2), 147.3 (C^6), 139.1 (C^4), 135.6 (Ph-o), 130.9 (Ph-p), 129.0 (Ph-i), 127.6 (Ph-m), 118.2 (C^5), 113.0 (C^3); $^{29}\text{Si}\{^1\text{H}\}$ NMR (CDCl_3): δ (ppm) –64.7.

Some crystals of the chloroform solvate $\text{PhSi}(\text{pyO})_3 \cdot \text{CHCl}_3$ ($\text{C}_{22}\text{H}_{18}\text{Cl}_3\text{N}_3\text{O}_3\text{Si}$) were obtained by recrystallization of the THF solvate in chloroform.

Compound $\text{PhGe}(\text{pyO})_3$ ($\text{C}_{21}\text{H}_{17}\text{GeN}_3\text{O}_3$). A Schlenk flask was charged with magnetic stirring bar and 2-hydroxypyridine (0.25 g, 2.63 mmol), then evacuated and set under Ar atmosphere prior to adding THF (5 mL) and triethylamine (0.40 g, 3.96 mmol). The resultant mixture was stirred at room temperature, and phenyltrichlorogermane (0.25 g, 0.97 mmol) was added dropwise via syringe through a septum. Upon completion, addition of the germane, a thick suspension was obtained. Therefore, further THF (2 mL) was added with

stirring, before the flask was stored at 5 °C for five days. Thereafter, the triethylamine hydrochloride precipitate was removed by filtration and washed with THF (3 mL). From the combined filtrate and washings, the solvent was removed under reduced pressure (condensation into a cold trap) to afford a viscous oily residue. This crude product was dissolved into THF (0.5 mL), then diethyl ether (1 mL) was added at room temperature, and the solution was stored undisturbed at room temperature for crystallization to commence. In the course of some days, crystals of PhGe(pyO)₃ formed. For enhanced yield, the flask was stored at −24 °C overnight prior to isolation of the product, which was achieved by decantation of the supernatant, washing with diethyl ether (1 mL), and drying in vacuum. Yield: 0.26 g (0.60 mmol, 68%). A single crystal was taken from this product for single-crystal X-ray diffraction analysis. Elemental analysis for C₂₁H₁₇GeN₃O₃ (431.99 g·mol^{−1}): C, 58.39%; H, 3.97%; N, 9.73%; found C, 58.23%; H, 4.38%; N, 9.79%. ¹H NMR (CDCl₃): δ (ppm) 8.13–8.09 (m, 2H, Ph-o), 7.86 (m, 3H, H⁶), 7.49 (m, 3H, H⁴), 7.44–7.34 (m, 3H, Ph-m/p), 6.80 (d, 3H, 8.3 Hz, H³), 6.70 (m, 3H, H⁵); ¹³C{¹H} NMR (CDCl₃): δ (ppm) 163.3 (C²), 145.9 (C⁶), 139.5 (C⁴), 134.3 (Ph-o), 133.8 (Ph-i), 130.8 (Ph-p), 128.2 (Ph-m), 116.2 (C⁵), 111.7 (C³).

Compound PhSn(pyO)₃ (C₂₁H₁₇N₃O₃Sn). A Schlenk flask was charged with magnetic stirring bar and 2-hydroxypyridine (2.03 g, 21.4 mmol), then evacuated and set under Ar atmosphere prior to adding THF (40 mL) and triethylamine (2.66 g, 26.3 mmol). The resultant mixture was stirred in an ice/ethanol bath (ca. −10 °C), and phenyltrichlorostannane (2.18 g, 7.21 mmol) was added dropwise via syringe through a septum. Upon completed addition of the stannane, the mixture was stored at 5 °C for five days, whereupon the triethylamine hydrochloride precipitate was removed by filtration and washed with THF (10 mL). From the combined filtrate and washings, the solvent was removed under reduced pressure (condensation into a cold trap) to afford a white solid residue. This crude product was recrystallized from hot THF. The colorless solid product thus obtained was filtered off, washed with THF (2 mL) and dried in vacuum. Yield: 2.13 g (4.46 mmol, 63%). A single crystal was taken from this product for single-crystal X-ray diffraction analysis. Elemental analysis for C₂₁H₁₇N₃O₃Sn (478.09 g·mol^{−1}): C, 52.76%; H, 3.58%; N, 8.79%; found C, 52.64%; H, 3.67%; N, 8.73%. ¹H NMR (CDCl₃): δ (ppm) 7.71–7.62 (m, 5H, Ph-o, H⁶), 7.57 (m, 3H, H⁴), 7.33–7.29 (m, 3H, Ph-m/p), 6.68 (d, 3H, 8.4 Hz, H³), 6.58 (m, 3H, H⁵); ¹³C{¹H} NMR (CDCl₃): δ (ppm) 167.0 (22 Hz, C²), 145.6 (1451 Hz, 1386 Hz, Ph-i), 142.3 (C⁶), 141.8 (18 Hz, C⁴), 133.7 (77 Hz, Ph-o), 129.5 (25 Hz, Ph-p), 128.6 (128 Hz, 122 Hz, Ph-m), 112.5 (C⁵), 111.3 (36 Hz, C³); ¹¹⁹Sn{¹H} NMR (CDCl₃): δ (ppm) −609; ¹¹⁹Sn CP/MAS NMR: δ_{iso} (ppm) −617.

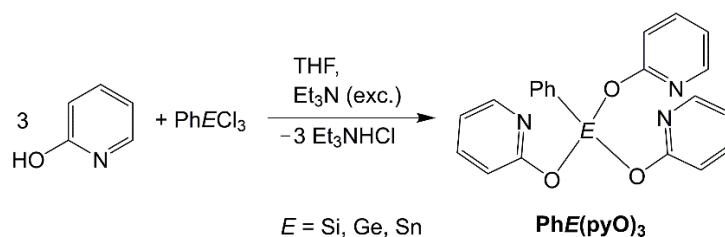
Note: For some ¹³C signals we observed ^{117/119}Sn satellites, the ¹¹⁷Sn and ¹¹⁹Sn contributions of which are not resolved. Therefore, the average *J*(^{117/119}Sn-¹³C) coupling constants are given in parentheses for those signals where applicable. For the pair of Ph-o and Ph-m ¹³C NMR signals (at 133.7 and 128.6 ppm) the larger *J*(^{117/119}Sn-¹³C) coupling is observed for the signal at 128.6 ppm. The assignment to o- and m-position is in accord with ¹³C NMR data of other phenyltin compounds, e.g., PhSn(ESiMe₂)₃SiMe (E = S, Se, Te), which give rise to signals of Ph-o and Ph-m carbon atoms around 134–135 ppm and 128–129 ppm, respectively [23], and for Me₃SnPh the same phenomenon of ³*J*(SnC) > ²*J*(SnC) has been reported [24].

3. Results and Discussion

3.1. Crystallographic Analysis of the Molecular Structures of PhE(pyO)₃ (E = Si, Ge, Sn)

Compounds PhE(pyO)₃ (E = Si, Ge, Sn) were synthesized from the respective chlorides PhECl₃ and 2-hydroxypyridine in THF with the aid of triethylamine as a sacrificial base (Scheme 1). In all cases, the crystalline products obtained were of sufficient quality for single-crystal X-ray diffraction analysis (Table A1). The crystallographically determined molecular structures of PhE(pyO)₃ (E = Si, Ge, Sn) are shown in Figure 2 and selected interatomic separations and bond angles are given in Table 1. Whereas the Ge- and Sn-compound crystallized from THF without including solvent of crystallization, compound PhSi(pyO)₃ crystallized as a THF solvate PhSi(pyO)₃·THF with severely disordered sol-

vent. Recrystallization from chloroform afforded an isomorphous solvate $\text{PhSi}(\text{pyO})_3 \cdot \text{CHCl}_3$, the disordered solvent of which could be refined in a satisfactory manner. As the structure models of $\text{PhSi}(\text{pyO})_3$ in the two solvates are of similar quality, and the molecular conformation of the silane in those structures is the same, the data from the solvate $\text{PhSi}(\text{pyO})_3 \cdot \text{CHCl}_3$ will be used in the further discussion as a representative example.



Scheme 1. Generic scheme of the syntheses of compounds $\text{PhSi}(\text{pyO})_3$, $\text{PhGe}(\text{pyO})_3$, and $\text{PhSn}(\text{pyO})_3$. The reactions were performed at room temperature for $\text{PhSi}(\text{pyO})_3$ and $\text{PhGe}(\text{pyO})_3$ and at -10°C for $\text{PhSn}(\text{pyO})_3$.

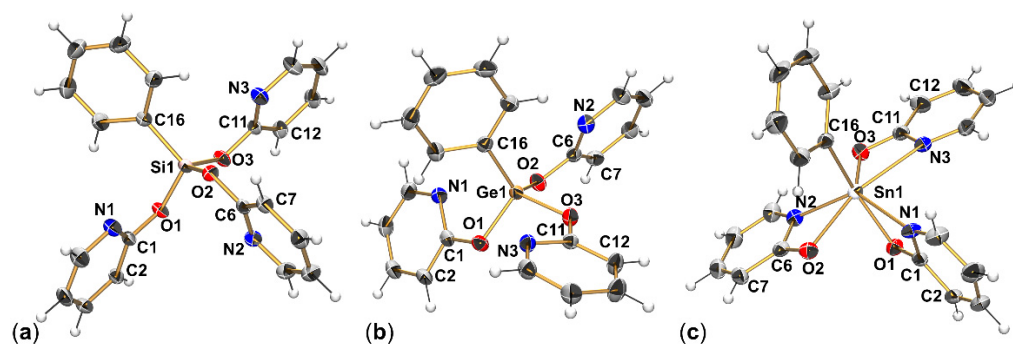


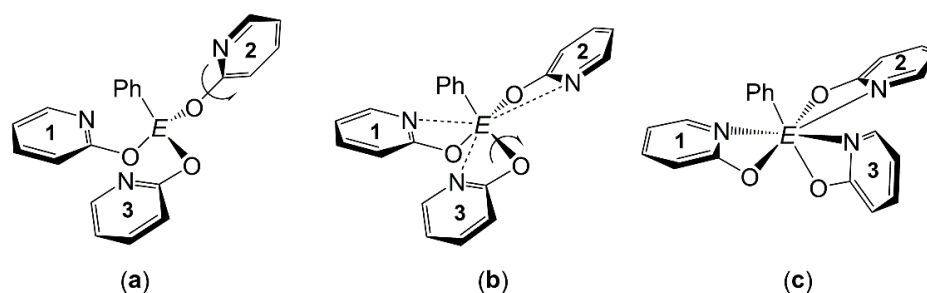
Figure 2. Molecular structures of (a) $\text{PhSi}(\text{pyO})_3$ (in the crystal structure of the solvate $\text{PhSi}(\text{pyO})_3 \cdot \text{CHCl}_3$), (b) $\text{PhGe}(\text{pyO})_3$, and (c) $\text{PhSn}(\text{pyO})_3$ with thermal displacement ellipsoids at the 50% probability level and labels of selected non-hydrogen atoms. Selected interatomic distances (\AA) and angles are listed in Table 1.

Table 1. Selected interatomic separations [\AA] and bond angles [deg] in the tetrel ($E = \text{Si, Ge, Sn}$) coordination spheres of $\text{PhSi}(\text{pyO})_3$, $\text{PhGe}(\text{pyO})_3$ and $\text{PhSn}(\text{pyO})_3$ and their pyO ligands.

Bond	$\text{PhSi}(\text{pyO})_3 \cdot \text{CHCl}_3$	$\text{PhGe}(\text{pyO})_3$	$\text{PhSn}(\text{pyO})_3$
$E1-O1$	1.640(1)	1.790(2)	2.120(2)
$E1-O2$	1.636(1)	1.777(2)	2.257(2)
$E1-O3$	1.642(1)	1.785(2)	2.133(2)
$E1-N1$	2.968(2)	2.789(2)	2.281(3)
$E1-N2$	3.002(2)	2.923(2)	2.212(3)
$E1-N3$	3.000(2)	2.908(2)	2.406(3)
$E1-C16$	1.842(2)	1.919(2)	2.138(2)
$O1-E1-O2$	115.85(6)	101.36(6)	84.64(9)
$O1-E1-O3$	96.91(6)	103.17(6)	93.00(9)
$O2-E1-O3$	112.54(6)	98.20(6)	138.85(9)
$O1-C1-N1$	117.50(13)	116.77(17)	113.0(3)
$O2-C6-N2$	117.30(13)	117.65(17)	113.9(3)
$O3-C11-N3$	117.45(13)	117.89(17)	113.5(3)
$O1-C1-C2$	117.55(13)	119.37(18)	126.2(3)
$O2-C6-C7$	117.96(13)	118.23(18)	126.7(3)
$O3-C11-C12$	117.47(13)	118.03(17)	124.3(3)

In compounds $\text{PhE}(\text{pyO})_3$ $E = \text{Si}, \text{Ge}$ the tetrel atom is essentially tetracoordinate, whereas in $\text{PhSn}(\text{pyO})_3$ the tin atom is clearly heptacoordinate within a pentagonal bipyramidal coordination sphere. In the latter, O1 and C16 occupy the axial positions (O1-Sn1-C16 $161.61(14)^\circ$), and the equatorial angles of pairs of neighboring bonds are $58.1(1)^\circ$ (O3-Sn1-N3) and $59.2(1)^\circ$ (O2-Sn1-N2) for the two chelate motifs and ca. 80° in the case of the remaining three angles spanned by O2,N1 ($80.4(1)^\circ$); O3,N2 ($79.7(1)^\circ$); N1,N3 ($80.4(1)^\circ$). Nonetheless, the molecular metrics of $\text{PhGe}(\text{pyO})_3$ already hint at a transition toward hypercoordination of the heavy tetrel atom. Whereas the $E\text{-O}$ bond lengths increase in an expected manner with an increasing atomic radius of E , the $E\cdots\text{N}$ separations already undergo some significant shortening (by more than 0.1 \AA on average) upon going from $E = \text{Si}$ to Ge . Thus, with respect to the N atom's van der Waals radius of 1.55 \AA and the tetrels' van der Waals radii of 2.10 (Si), 2.11 (Ge), and 2.17 \AA (Sn) [25], the average $E\cdots\text{N}$ separations are 81.9%, 78.5%, and 61.8% of the sum of van der Waals radii for the Si, Ge, and Sn compound, respectively. Further evidence for pronounced $E\cdots\text{N}$ attraction upon going from $E = \text{Si}$ to Ge can be found in the O-C-N angle deformation of all pyridine-2-olate groups. Whereas in the silicon compound the O-C-N angles and their corresponding O-C-C angles are very similar (both ca. 117.5°), the O-C-N angles in the Ge compound are slightly smaller than the corresponding O-C-C angles, thus indicating the pronounced attractive $\text{Ge}\cdots\text{N}$ interaction. At the Ge atom in compound $\text{PhGe}(\text{pyO})_3$, the trend of bond angles adheres to VSEPR, i.e., within the GeC_1O_3 coordination sphere, all O-Ge-O angles are smaller than the tetrahedral angle. In sharp contrast, $\text{PhSi}(\text{pyO})_3$ features one very small O-Si-O angle (O1-Si1-O3 $96.91(6)^\circ$), whereas the other two O-Si-O angles ($112.54(6)$ and $115.85(6)^\circ$) are noticeably wider than the tetrahedral angle. (Similar features are found in compound $\text{MeSi}(\text{pyO})_3$ [2].) This phenomenon can be attributed to the molecular conformation of $\text{PhSi}(\text{pyO})_3$ with respect to its enhanced coordination sphere (i.e., [4+3]-coordination). In the case of $\text{PhGe}(\text{pyO})_3$, each of the pyridine N atoms is capping a tetrahedral face *trans* to a Ge-O bond and thus widens the O-Ge-C angles. The tetrahedral face *trans* to the Ge-C bond lacks this effect and thus allows for mutual shrinkage of the O-Ge-O angles (sum of O-Ge-O angles 302.7°). In the case of $\text{PhSi}(\text{pyO})_3$, N2 is capping the tetrahedral face *trans* to the Si-C bond and thus widens the O-Si-O angles (sum of O-Si-O angles 325.3°). As the tetrahedral face *trans* to Si1-O2 is devoid of a remote donor atom (thus not exerting any additional widening to angle O1-Si1-O3), and the capping of tetrahedral faces by N1 and N3 enforces further widening of angles O1-Si1-O2 and O3-Si1-O2, respectively, bond angle O1-Si1-O3 becomes particularly narrow. Noteworthy, with respect to the overall deformation of the tetrahedral coordination sphere about the tetrel atom, the geometry parameter τ_4 [26] (Si: 0.91, Ge: 0.83) indicates particular deformation in the case of the Ge compound. It originates from a noticeably wide angle O2-Ge1-C16 ($124.3(1)^\circ$). This feature arises from a C-H \cdots N2 contact, in which a phenyl ortho-H atom interferes with pyridine atom N2 and thus competes with the capping of the tetrahedral face *trans* to Ge1-O1 by atom N2.

In addition to visualizing the conformational differences between the two [4+3]-coordinate tetrel compounds $\text{PhSi}(\text{pyO})_3$ and $\text{PhGe}(\text{pyO})_3$, the view in Figure 2 demonstrates the relationship of the conformation of $\text{PhGe}(\text{pyO})_3$ and the conformation of the pentagonal bipyramidal Sn-coordination compound $\text{PhSn}(\text{pyO})_3$. Scheme 2 illustrates this hypothetical transition, starting from the molecular conformation of $\text{PhGe}(\text{pyO})_3$ (Scheme 2a). In addition to the N atoms approaching the tetrel E , partial rotation of the pyO ligands indexed with "2" and "3" about the bonds shown with rotation arrows in Scheme 2a,b affords the molecular configuration of $\text{PhSn}(\text{pyO})_3$ (Scheme 2c).



Scheme 2. Schematic representation of the ligand motion (of corresponding pyO moieties “1”, “2” and “3”) which relates the molecular conformations of PhGe(pyO)₃ (starting point (a)) and PhSn(pyO)₃ (represented by (c)) to one another via (b).

The increasing intensity of N⋯E coordination in the series $E = \text{Si} < \text{Ge} < \text{Sn}$ is also reflected by the systematic changes in corresponding bond lengths within the pyO moieties (Table A2). Whereas most bond length differences merely allow for a vague hint at a trend (the changes, albeit seemingly systematic, are not significant within the boundaries of the standard deviations), significant shortening of the C–O bonds and, to a lesser extent, lengthening of the adjacent C–N bond is observed. Thus, the response of the pyO ligand’s C–C bond backbone to mono- vs. bidentate coordination is less pronounced than the response of the related *N*-oxide (1-oxy-2-pyridinone, OPO) in compound $(t\text{Bu})_2\text{Si}(\text{OPO})_2$, which features both a monodentate and a chelating OPO moiety within the same molecule [27].

The molecular conformation of PhSn(pyO)₃ requires some further discussion in context with the literature data. Even though this is the first crystallographically characterized “simple” stannane with more than one pyO substituent, some related compounds of the type RSn(pyS)₃ (pyS = pyridine-2-thiolate) have been reported and characterized crystallographically (with R = *p*-tolyl [28], Me and Ph [29]). In these compounds, the Sn atom is also heptacoordinate within an almost pentagonal bipyramidal coordination sphere, and the hydrocarbonyl group as well as one chelate ligand’s chalcogen atom occupy axial positions. Their equatorial chelate ligands, however, are arranged in a *cis* fashion (thus giving rise to an equatorial N,N,N,S,S atom sequence), whereas in PhSn(pyO)₃ *trans*-arrangement of the two equatorial chelates is found (and an equatorial N,N,O,N,O atom sequence arises therefrom). With a different (O,N)-bidentate ligand system (ox = oxinate, 8-quinolinolate), compound RSn(ox)₃ (R = 4-chlorophenyl) with pentagonal bipyramidal Sn coordination sphere has been reported [30]. The conformation of this compound is less related to PhSn(pyO)₃ as it exhibits two differences: mutual *cis*-arrangement of the equatorial chelates and N-axial-O-equatorial arrangement of the third chelate ligand. Figure 3 illustrates this conformational difference.

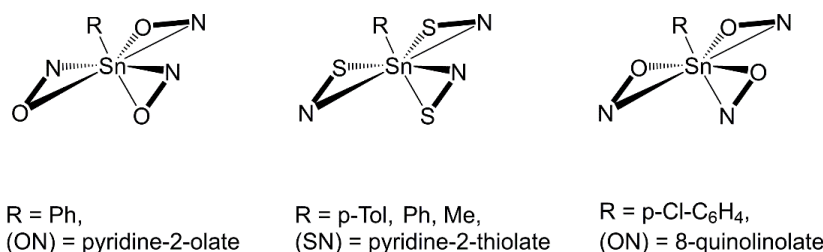


Figure 3. Generic illustration of the conformational difference between PhSn(pyO)₃, related pyridine-2-thiolates RSn(pyS)₃ [28,29] and 8-quinolinolate (4-Cl-C₆H₄)Sn(ox)₃ [30]. The motifs “N–O” and “N–S” serve as abbreviations of the different bidentate (N,O)- and (N,S)-donor ligands.

Apart from the comparison of PhSn(pyO)₃ with more or less related organotin-tris(chelates) with pentagonal bipyramidal Sn coordination sphere, the context of (Si,Ge,Sn)-hypercoordination within related four-membered (E,O,C,N)-chelate rings formed by mono-anionic chelators and tetravalent tetrels must be addressed. A search in the Cambridge

Crystal Structure Database [7] yielded a very limited number of (Si,Ge,Sn)-compounds with hypercoordinate (i.e., coordination number greater than four) tetrel atoms and such monoanionic (O,N)-chelating ligands. In the case of silicon, the portfolio is limited to three different compounds with hexacoordinate Si atoms, VII [31], VIII [32], and IX [33] (Figure 4). Enhanced Lewis acidity of the Si atom (caused by one or combinations of the parameter(s) such as small rings, electron-withdrawing substituents, and the cationic nature of the complex) may be an essential prerequisite. No representatives of hypercoordinate Ge compounds were found. Even the portfolio of structurally characterized hypercoordinate tetravalent tin compounds with this structural motif is very limited. For tin coordination numbers 6, 7, and 8, no appropriate hits were encountered. For Sn coordination number 7 only one multinuclear tin complex was found which features an (Sn,O,C,N)-chelate within a greater system of charge-delocalized multidentate ligands [34]. Even with tin coordination number 5, only two representatives (compounds X) were encountered. Interestingly, their four-membered (Sn,O,C,N)-chelates are derived from the pyridine-2-olate system [35].

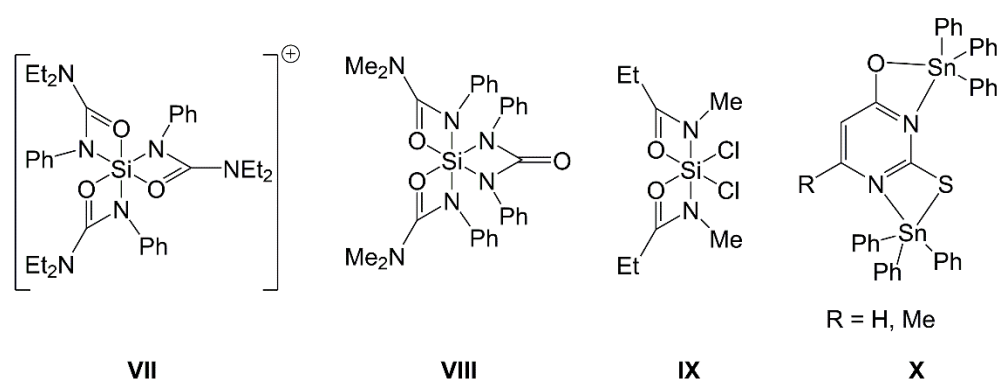


Figure 4. Literature known examples of structurally confirmed hypercoordinate tetravalent tetrel (*E*) compounds (compounds VII–X) with (*E,O,C,N*)-four-membered rings formed by mono-anionic (*O,N*)-chelating ligands.

In summary, structural characterization of hypercoordinate tetrels with four-membered (*E,O,C,N*)-chelates by mono-anionic chelators is still a rather unexplored field. With respect to pyridine-2-olate as a simple representative of such ligands, we may conclude that in the case of silicon compounds the lower tendency of the light tetrel toward hypercoordination can be seen as the major reason, as shown with $\text{PhSi}(\text{pyO})_3$ and other examples [1–3]. In the case of Sn compounds, however, the lack of crystallographic evidence for solely Sn–O bound pyridine-2-olates with non-coordinating pyridine N atom [7] and the previously mentioned lack of structurally characterized Sn–pyO-chelates is highlighting a field of tetrel coordination chemistry yet to be explored.

3.2. NMR Spectroscopic Analyses of $\text{PhE}(\text{pyO})_3$ (*E* = Si, Ge, Sn)

Compounds $\text{PhE}(\text{pyO})_3$ (*E* = Si, Ge, Sn) were characterized by NMR spectroscopy in CDCl_3 solution and, in the case of $\text{PhSn}(\text{pyO})_3$, with ^{119}Sn solid-state NMR spectroscopy.

In the CDCl_3 solution, the Si atom of compound $\text{PhSi}(\text{pyO})_3$ is tetracoordinate, indicated by $\delta^{29}\text{Si} = -64.7$ ppm. This signal is upfield shifted with respect to that of the corresponding methyl compound $\text{MeSi}(\text{pyO})_3$ ($\delta^{29}\text{Si} = -46.5$ ppm [2]), which is a common observation with pairs of corresponding PhSi and MeSi compounds (e.g., $\text{PhSi}(\text{OEt})_3$ $\delta^{29}\text{Si} = -57.8$ ppm [36], $\text{MeSi}(\text{OEt})_3$ $\delta^{29}\text{Si} = -44.5$ ppm [37]). In principle, compound $\text{PhSi}(\text{pyO})_3$ has a similar ^{29}Si NMR shift as the tetracoordinate phenyl silicon compound $\text{PhSi}(\text{OEt})_3$.

For compound $\text{PhSn}(\text{pyO})_3$ the ^{119}Sn NMR shifts were recorded in the solid state (−617 ppm, Figure 5) as well as in CDCl_3 at different temperatures (20 °C: −609 ppm, −40 °C: −614 ppm). These chemical shifts are basically speaking for retention of the tin coordination number 7 in the CDCl_3 solution. Furthermore, these shifts are similar to those

of other stannanes with heptacoordinate Sn atom and ArylSn(O,N)₃ coordination, e.g., *p*-TolSn(quinoline-8-olate)₃ (−611 ppm), *p*-TolSn(pyridine-2-carboxylate)₃ (−620 ppm) [30].

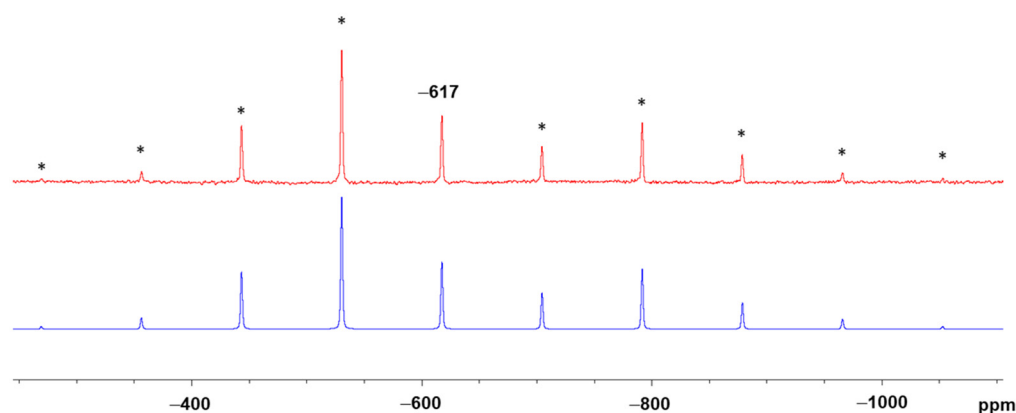


Figure 5. ²⁹Si MAS NMR spectrum of PhSn(pyO)₃ recorded at a spinning frequency of 13 kHz (top, red trace) and simulated spectrum using the CSA tensor data derived from the experimental spectrum (bottom, blue trace). The asterisked (*) peaks are spinning sidebands. CSA tensor data: δ_{iso} −617.4 ppm, δ_{11} −393.5 ppm, δ_{22} −502.2 ppm, δ_{33} −956.5 ppm, Ω 563 ppm, κ 0.61.

In the ¹H and ¹³C NMR spectra of each of the compounds PhE(pyO)₃ (E = Si, Ge, Sn), the three pyO moieties give rise to one set of four (¹H) or five (¹³C) signals, which was expected at least for the Si compound in accord with previously reported pyO-functionalized silanes [2,3]. In the case of compound PhSn(pyO)₃, it confirms that the SnCN₃O₃ coordination sphere itself is highly flexible and undergoes rapid exchange processes. Even cooling to −40 °C did not cause any signal broadening or decoalescence effects (Figure 6).

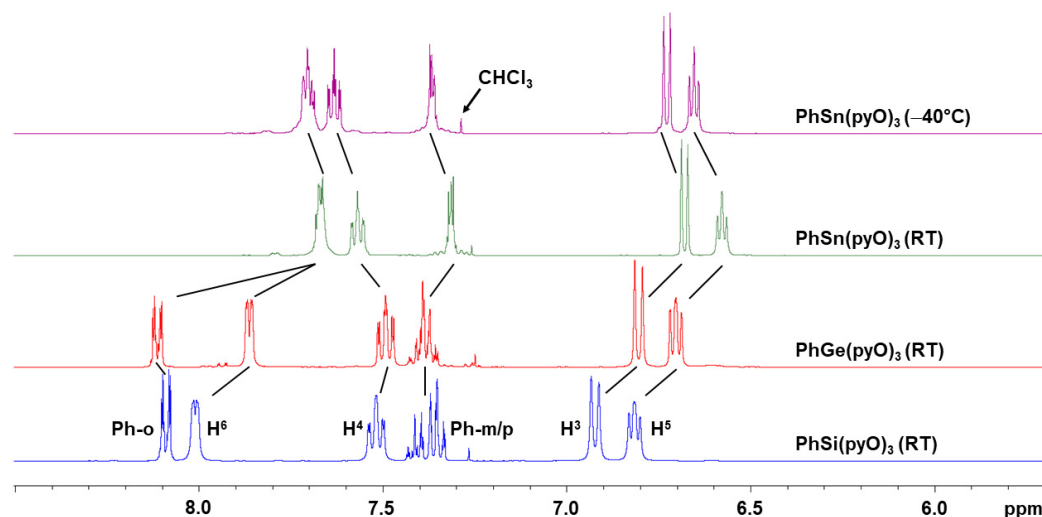


Figure 6. Section of the ¹H NMR spectra of CDCl₃ solutions of (from bottom to top) PhSi(pyO)₃, PhGe(pyO)₃, and PhSn(pyO)₃ at room temperature as well as of PhSn(pyO)₃ at −40 °C. The spectra are internally referenced to SiMe₄ (cf. spectra shown in Figures S1, S4, and S6 in the supplementary material).

To evaluate the pyO@Ge coordination chemistry of PhGe(pyO)₃ in CDCl₃ solution, a comparison of ¹H and ¹³C NMR spectra of this compound with those of the lighter and heavier congener was engaged. In ¹³C NMR spectra, it was found that the C² and C⁶ positions of the pyO groups are highly responsive to coordinative changes at the N atom. In the spectrum of a CDCl₃ solution of compound PhP(pyO)₂ [13] the signals of interest emerge at 161.8 ppm (C²) and 147.4 ppm (C⁶). The spectrum of the related compound PhSb(pyO)₂ [38], which exhibits pronounced Sb⋯N attraction, exhibits the

corresponding signals at 167.0 ppm (C^2) and 140.6 ppm (C^6). The corresponding signals of the related arsenic compound $\text{PhAs}(\text{pyO})_2$ [39] emerge at intermediate positions. Even though this trend may also be influenced by electronic effects through the $E\text{--O--C}_5\text{N}$ σ - and π -bond system (originating from different $E\text{--O}$ bonds caused by the different elements E), the relevance of the electronic effects caused by $\text{N}\rightarrow$ tetrel coordination is underlined by corresponding data of a set of literature known pyridine-2-thiolate (pyS) compounds [3,40,41], which show that the same trends are observed for C^2 and C^6 , but these trends are more responsive to hypercoordination ($E(\text{S},\text{N})$ -chelation vs. absence of $E\cdots\text{N}$ coordination) rather than to the element E itself (cf. Table A3).

The ^1H and ^{13}C NMR spectra of compound $\text{PhGe}(\text{pyO})_3$ in CDCl_3 solution resemble both the signal patterns (^1H coupling patterns) and the chemical shifts of corresponding signals (both ^1H and ^{13}C) of the related silicon compound. For a comparison of their ^1H NMR signals, see Figure 6. For the series of spectra of $\text{PhE}(\text{pyO})_3$ ($E = \text{Si}, \text{Ge}, \text{Sn}$) recorded at room temperature, systematic shift trends are observed for corresponding ^1H signals of the pyO moieties. The upfield shift of the ^1H NMR signal of the pyO protons in position 6 from $E = \text{Si}$ via Ge to Sn is the most prominent trend among their pyO ^1H signals and thus underlines the changes in $\text{N}\cdots E$ coordination, which can be derived from ^{13}C NMR data (Table 2). A trend toward hypercoordination of the Ge atom is indicated by the ^{13}C NMR shifts of the pyO carbon atoms in positions 2 and 6. Their signals are further downfield shifted (C^2 , by 3 ppm) and upfield shifted (C^6 , by 1.4 ppm) in the Ge compound.

Table 2. ^{13}C NMR shifts of C^2 and C^6 of the pyridine-2-olate (pyO) ligands of compounds $\text{PhE}(\text{pyO})_3$ in CDCl_3 .

Compound	$E\cdots\text{N}(\text{pyS})$ Coordination? ¹	$\delta^{13}\text{C}(C^2)$	$\delta^{13}\text{C}(C^6)$
$\text{PhSi}(\text{pyO})_3$	0	160.3	147.3
$\text{PhGe}(\text{pyO})_3$	intermediate	163.3	145.9
$\text{PhSn}(\text{pyO})_3$	1	167.0	141.8

¹ According to the number of pyO groups in the molecule and the coordination number of E , all pyO groups (1) or no pyO groups (0) establish $E\cdots\text{N}$ coordination. The ^{13}C NMR shift trends indicate intermediate $E\cdots\text{N}$ coordination for the Ge compound.

4. Conclusions

In general, compounds such as the herein presented set $\text{PhE}(\text{pyO})_3$ represent potential starting materials for the syntheses of heteronuclear complexes. For compounds such as $\text{MeSi}(\text{pyO})_3$ [2], $\text{Si}(7\text{-azaindoly})_4$ [42], $\text{ClSi}(\text{mt})_3$ [43], $\text{Si}(\text{mt})_4$ [44], $\text{FPhE}(\text{o-C}_6\text{H}_4\text{-P}^i\text{Pr}_2)_2$ ($E = \text{Si}, \text{Sn}$) [45], $\text{FE}(\text{o-C}_6\text{H}_4\text{-PPh}_2)_3$ ($E = \text{Si}, \text{Ge}, \text{Sn}$) [46], $\text{FSi}(\text{CH}_2\text{CH}_2\text{PMe}_2)_2$ [47], $\text{MeSi}(\text{OCH}_2\text{PMe}_2)_2(\text{CH}_2\text{CH}_2\text{PMe}_2)$ [48] it has been shown that their dangling donor atoms (N, S, P) may bind to transition metals and, in some cases, foster establishing of formally dative bonding of the transition metal to the tetrel. As dangling donor arms of their potentially bidentate substituents may be essential for binding to another metal atom (because of the absence of other reactive groups within the molecule), compounds $\text{PhSi}(\text{pyO})_3$ and $\text{PhGe}(\text{pyO})_3$ with their absent or poor $E\cdots\text{N}$ coordination appear more suitable for that purpose than the related tin compound, in which the N atoms are engaged in a competing situation, i.e., $\text{Sn}\cdots\text{N}$ coordination also in solution. The flexibility/mobility of the Sn coordination sphere, however, may still render compounds such as $\text{PhSn}(\text{pyO})_3$ suitable for the same purpose. Detailed studies of the ligand qualities of Ge- and Sn-pyO-compounds are yet to be performed. For compounds of the type $\text{RSi}(\text{pyO})_3$ we had already confirmed the suitability as a ligand for Cu(I) in the case of $\text{R} = \text{Me}$ [2], and a study of related silanes ($\text{R} = \text{Ph}, \text{Benzyl}, \text{Allyl}$) is currently underway.

Supplementary Materials: The following supporting information can be downloaded at: <https://www.mdpi.com/article/10.3390/cryst12121802/s1>: NMR spectra (^1H , $^{13}\text{C}\{^1\text{H}\}$) and, where applicable, $^{29}\text{Si}\{^1\text{H}\}$ or $^{119}\text{Sn}\{^1\text{H}\}$ of CDCl_3 solutions of compounds $\text{PhSi}(\text{pyO})_3$ (Figures S1–S3), $\text{PhGe}(\text{pyO})_3$ (Figures S4, S5), and $\text{PhSn}(\text{pyO})_3$ (Figures S6–S9).

Author Contributions: Conceptualization, J.W.; investigation, S.K., E.B., and J.W.; writing—original draft preparation, J.W.; writing—review and editing, E.B. and J.W.; visualization, J.W.; supervision, J.W. All authors have read and agreed to the published version of the manuscript.

Funding: This research received no external funding.

Institutional Review Board Statement: Not applicable.

Informed Consent Statement: Not applicable.

Data Availability Statement: Not applicable.

Acknowledgments: The authors are grateful to Beate Kutzner, Franziska Gründler, and Mareike Weigel (TU Bergakademie Freiberg, Institut für Anorganische Chemie) for solution NMR (B.K.) and elemental microanalysis service (F.G., M.W.), and to the students Alexandra Becker and Arthur Hentschel (TU Bergakademie Freiberg) for preparing additional batches of compound $\text{PhSi}(\text{pyO})_3 \cdot \text{THF}$.

Conflicts of Interest: The authors declare no conflict of interest.

Appendix A

Table A1. Crystallographic data from data collection and refinement for $\text{PhSi}(\text{pyO})_3$ (its THF solvate, and chloroform solvate), $\text{PhGe}(\text{pyO})_3$, and $\text{PhSn}(\text{pyO})_3$.

Parameter	$\text{PhSi}(\text{pyO})_3 \cdot \text{THF}$ ¹	$\text{PhSi}(\text{pyO})_3 \cdot \text{CHCl}_3$ ²	$\text{PhGe}(\text{pyO})_3$	$\text{PhSn}(\text{pyO})_3$ ³
Formula	$\text{C}_{25}\text{H}_{25}\text{N}_3\text{O}_4\text{Si}$	$\text{C}_{22}\text{H}_{18}\text{Cl}_3\text{N}_3\text{S}_3\text{Si}$	$\text{C}_{21}\text{H}_{17}\text{GeN}_3\text{O}_3$	$\text{C}_{21}\text{H}_{17}\text{N}_3\text{O}_3\text{Sn}$
M_r	459.57	506.83	431.96	478.07
T (K)	200(2)	180(2)	180(2)	150(2)
λ (Å)	0.71073	0.71073	0.71073	0.71073
Crystal system	monoclinic	monoclinic	triclinic	monoclinic
Space group	$P2_1/c$	$P2_1/c$	$P\bar{1}$	$P2_1$
a (Å)	12.1634(6)	12.2304(4)	9.7609(3)	8.4129(3)
b (Å)	17.0246(10)	16.8989(4)	9.7775(3)	10.9605(2)
c (Å)	11.4268(7)	11.3681(3)	9.8668(3)	10.8580(3)
α (°)	90	90	82.957(2)	90
β (°)	101.450(4)	101.160(2)	83.434(2)	98.385(2)
γ (°)	90	90	86.564(2)	90
V (Å ³)	2319.1(2)	2395.13(11)	927.42(5)	990.51(5)
Z	4	4	2	2
ρ_{calc} (g·cm ⁻³)	1.32	1.46	1.55	1.60
$\mu_{\text{MoK}\alpha}$ (mm ⁻¹)	0.1	0.5	1.7	1.3
$F(000)$	968	1040	440	476
θ_{max} (°), R_{int}	28.0, 0.0243	28.0, 0.0454	28.0, 0.0428	29.0, 0.0270
Completeness	99.8%	99.9%	100%	99.9%
Reflns collected	15,889	26,422	24,367	56,321
Reflns unique	5587	5563	4480	5258
Restraints	0	73	0	1
Parameters	253	353	254	254
GoF	1.072	1.053	1.077	1.256
$R1, wR2$ [$I > 2\sigma(I)$]	0.0425, 0.1078	0.0420, 0.0983	0.0310, 0.0687	0.0184, 0.0416
$R1, wR2$ (all data)	0.0639, 0.1203	0.0570, 0.1059	0.0368, 0.0708	0.0203, 0.0433
Largest peak/hole (e·Å ⁻³)	0.23, -0.39	0.30, -0.34	0.30, -0.50	0.93, -0.96

¹ The solvent molecule (THF) was severely disordered over many sites and could not be refined in a satisfactory manner. Therefore, the solvent was treated with SQUEEZE as implemented in PLATON [49–51]. This procedure detected per unit cell, solvent accessible volume of 562 Å³, and contributions of 160 electrons therein (well in accord with 160 electrons for the four THF molecules per unit cell, which have been omitted from refinement).

² The solvent molecule (chloroform) was refined disordered over three sites with site occupancy factors 0.269(6), 0.316(4) and 0.415(6). ³ The absolute structure parameter χ_{Flack} of this non-centrosymmetric structure refined to -0.035(6).

Table A2. Bond lengths [Å] of the pyridine-2-olate moieties in PhSi(pyO)₃ · CHCl₃, PhGe(pyO)₃ and PhSn(pyO)₃.

Bond ¹	PhSi(pyO) ₃ · CHCl ₃	PhGe(pyO) ₃	PhSn(pyO) ₃
O1–C1	1.362(2)	1.350(2)	1.314(4)
O2–C6	1.364(2)	1.350(2)	1.288(4)
O3–C11	1.360(2)	1.350(2)	1.315(4)
N1–C1	1.322(2)	1.327(3)	1.347(4)
N2–C6	1.321(2)	1.324(3)	1.348(4)
N3–C11	1.319(2)	1.324(3)	1.337(4)
C1–C2	1.386(2)	1.391(3)	1.408(4)
C5–C6	1.387(2)	1.389(3)	1.421(4)
C11–C12	1.392(2)	1.391(3)	1.403(4)
C2–C3	1.379(2)	1.379(3)	1.375(5)
C7–C8	1.379(2)	1.376(3)	1.368(5)
C12–C13	1.379(2)	1.374(3)	1.380(6)
C3–C4	1.385(3)	1.387(3)	1.399(5)
C8–C9	1.386(2)	1.388(3)	1.394(6)
C13–C14	1.384(3)	1.389(3)	1.391(6)
C4–C5	1.372(3)	1.376(3)	1.370(5)
C9–C10	1.371(3)	1.375(3)	1.379(5)
C14–C15	1.374(3)	1.372(3)	1.378(6)
N1–C5	1.345(2)	1.343(3)	1.341(4)
N2–C10	1.349(2)	1.349(3)	1.347(4)
N3–C15	1.347(2)	1.347(3)	1.353(4)

¹ For clarity of presentation, groups of corresponding bonds within the set of individual ligands of each molecule were summarized within a block of the same shading.

Table A3. ¹³C NMR shifts of C² and C⁶ of the pyridine-2-thiolate (pyS) ligands of a series of related silicon and tin compounds in CDCl₃ or CD₂Cl₂ solution.

Compound	E	Solvent	E···N(pyS) Coordination? ¹	δ ¹³ C(C2)	δ ¹³ C(C6)
PhClSi(pyS) ₂ [40]	Si	CD ₂ Cl ₂	1	167.5	140.8
MeClSi(pyS) ₂ [40]	Si	CD ₂ Cl ₂	1	168.1	140.4
Si(pyS) ₄ [41]	Si	CDCl ₃	0.5	163.4	144.7
Sn(pyS) ₄ [41]	Sn	CDCl ₃	0.5	162.9	145.7
Ph ₂ Si(pyS) ₂ [3]	Si	CDCl ₃	0	158.1	147.5
Me ₂ Si(pyS) ₂ [3]	Si	CDCl ₃	0	158.7	148.8

¹ According to the number of pyS groups in the molecule and the coordination number of E, all pyS groups (1) or no pyS groups (0) establish E···N coordination. In the case of compounds E(pyS)₄, the coordination number of E is 6. In these compounds, two E···N coordinating and two non-E···N-coordinating pyS groups exchange in a dynamic equilibrium (thus, a formal contribution of 0.5 of each pyS group to the overall E···N coordination arises therefrom).

References

- Kazimierczuk, K.; Dołęga, A. Department of A. Synthesis and structural characterization of new cyclic siloxane with functionalized organic substituents. *Phosphorus Sulfur Silicon Relat. Elem.* **2017**, *192*, 1140–1143. [[CrossRef](#)]
- Ehrlich, L.; Gericke, R.; Brendler, E.; Wagler, J. (2-Pyridyloxy)silanes as Ligands in Transition Metal Coordination Chemistry. *Inorganics* **2018**, *6*, 119. [[CrossRef](#)]
- Seidel, A.; Weigel, M.; Ehrlich, L.; Gericke, R.; Brendler, E.; Wagler, J. Molecular Structures of the Silicon Pyridine-2-(thi)olates Me₃Si(pyX), Me₂Si(pyX)₂ and Ph₂Si(pyX)₂ (py = 2-Pyridyl, X = O, S), and Their Intra- and Intermolecular Ligand Exchange in Solution. *Crystals* **2022**, *12*, 1054. [[CrossRef](#)]
- Sun, J.; Ou, C.; Wang, C.; Uchiyama, M.; Deng, L. Silane-Functionalized N-Heterocyclic Carbene–Cobalt Complexes Containing a Five-Coordinate Silicon with a Covalent Co–Si Bond. *Organometallics* **2015**, *34*, 1546–1551. [[CrossRef](#)]
- Julián, A.; Garcés, K.; Lalrempuia, R.; Jaseer, E.A.; García-Orduña, P.; Fernández-Alvarez, F.J.; Lahoz, F.J.; Oro, L.A. Reactivity of Ir–NSiN Complexes: Ir-Catalyzed Dehydrogenative Silylation of Carboxylic Acids. *ChemCatChem* **2018**, *10*, 1027–1034. [[CrossRef](#)]
- Kanno, Y.; Komuro, T.; Tobita, H. Direct Conversion of a Si–C(aryl) Bond to Si–Heteroatom Bonds in the Reactions of η³-α-Silabenzyl Molybdenum and Tungsten Complexes with 2-Substituted Pyridines. *Organometallics* **2015**, *34*, 3699–3705. [[CrossRef](#)]
- This refers to a search in the Cambridge Structure Database using ConQuest version 2022.2.0.

8. Hadjikakou, K.; Jurkschat, K.; Schürmann, M. Novel organotin(IV) compounds derived from bis(organostannyl)methanes: Synthesis and crystal structures of bis[diphenyl(pyridin-2-onato)stannyl]methane and bis[bromophenyl(pyrimidine-2-thionato)stannyl]methane · C₇H₈. *J. Organomet. Chem.* **2006**, *691*, 1637–1642. [[CrossRef](#)]
9. Ma, C.; Li, Q.; Zhang, R. A novel self-assembling of mixed tri- and dibutyltin macrocyclic complex with solvothermal synthesis method. *Inorg. Chim. Acta* **2009**, *362*, 2937–2940. [[CrossRef](#)]
10. Haribabu, J.; Tamura, Y.; Yokoi, K.; Balachandran, C.; Umezawa, M.; Tsuchiya, K.; Yamada, Y.; Karvembu, R.; Aoki, S. Synthesis and Anticancer Properties of Bis- and Mono(cationic peptide) Hybrids of Cyclometalated Iridium(III) Complexes: Effect of the Number of Peptide Units on Anticancer Activity. *Eur. J. Inorg. Chem.* **2021**, *2021*, 1796–1814. [[CrossRef](#)]
11. Zhou, J.; Yu, G.; Yang, J.; Shi, B.; Ye, B.; Wang, M.; Huang, F.; Stang, P.J. Polymeric Nanoparticles Integrated from Discrete Organoplatinum(II) Metallacycle by Stepwise Post-assembly Polymerization for Synergistic Cancer Therapy. *Chem. Mater.* **2020**, *32*, 4564–4573. [[CrossRef](#)]
12. Yusof, E.N.M.; Ravoo, T.B.S.A.; Page, A.J. Cytotoxicity of Tin(IV)-based compounds: A review. *Polyhedron* **2021**, *198*, 115069. [[CrossRef](#)]
13. Gericke, R.; Wagler, J. Ruthenium complexes of phosphino derivatives of carboxylic amides: Synthesis and characterization of tridentate P₂E₂ and tetradentate P₂E₃ (E = N,O) ligands and their reactivity towards [RuCl₂(PPh₃)₃]. *Polyhedron* **2017**, *125*, 57–67. [[CrossRef](#)]
14. Herzfeld, J.; Berger, A.E. Sideband intensities in NMR spectra of samples spinning at the magic angles. *J. Chem. Phys.* **1980**, *73*, 6021–6030. [[CrossRef](#)]
15. Mason, J. Conventions for the reporting of nuclear magnetic shielding (or shift) tensors suggest by participants in the NATO AEW in NMR Shielding Constants at the University of Maryland, College Park, July 1992. *Solid State Nucl. Magn. Reson.* **1993**, *2*, 285–288. [[CrossRef](#)] [[PubMed](#)]
16. Sheldrick, G.M. *Program for the Solution of Crystal Structures*; SHELXS-97; University of Göttingen: Göttingen, Germany, 1997.
17. Sheldrick, G.M. SHELXT—Integrated space-group and crystal-structure determination. *Acta Crystallogr. A* **2015**, *71*, 3–8. [[CrossRef](#)] [[PubMed](#)]
18. Sheldrick, G.M. *Program for the Refinement of Crystal Structures*; SHELXL-2014/7; University of Göttingen: Göttingen, Germany, 2014.
19. Sheldrick, G.M. A short history of SHELX. *Acta Crystallogr. A* **2008**, *64*, 112–122. [[CrossRef](#)]
20. Farrugia, L.J. ORTEP-3 for windows—A version of ORTEP-III with a graphical user interface (GUI). *J. Appl. Crystallogr.* **1997**, *30*, 565. [[CrossRef](#)]
21. Farrugia, L.J. WinGX and ORTEP for Windows: An update. *J. Appl. Crystallogr.* **2012**, *45*, 849–854. [[CrossRef](#)]
22. POV-RAY (Version 3.7), Trademark of Persistence of Vision Raytracer Pty. Ltd., Williamstown, Victoria (Australia). Copyright Hallam Oaks Pty. Ltd., 1994–2004. Available online: <http://www.povray.org/download/> (accessed on 28 June 2021).
23. Herzog, U.; Rheinwald, G. Novel Chalcogenides of Silicon with Bicyclo[2.2.2]octane Skeletons, MeSi(SiMe₂E)₃MR (E = S, Se, Te; M = Si, Ge, Sn; R = Me, Ph). *Organometallics* **2001**, *20*, 5369–5374. [[CrossRef](#)]
24. Schaeffer, C.D., Jr.; Zuckerman, J.J. Pulsed fourier transform NMR of substituted aryltrimethyltin derivatives: II. (¹¹⁹Sn-¹³C) coupling constants and ¹³C chemical shifts of meta- and para-derivatives. *J. Organomet. Chem.* **1973**, *55*, 97–110. [[CrossRef](#)]
25. Mantina, M.; Chamberlin, A.C.; Valero, R.; Cramer, C.J.; Truhlar, D.G. Consistent van der Waals Radii for the Whole Main Group. *J. Phys. Chem. A* **2009**, *113*, 5806–5812. [[CrossRef](#)] [[PubMed](#)]
26. Okuniewski, A.; Rosiak, D.; Chojnaki, J.; Becker, B. Coordination polymers and molecular structures among complexes of mercury(II) halides with selected 1-benzoylthioureas. *Polyhedron* **2015**, *90*, 47–57. [[CrossRef](#)]
27. Kraft, B.M.; Brennessel, W.W. Chelation and Stereodynamic Equilibria in Neutral Hypercoordinate Organosilicon Complexes of 1-Hydroxy-2-pyridinone. *Organometallics* **2014**, *33*, 158–171. [[CrossRef](#)]
28. Schürmann, M.; Huber, F. Tris(2-pyridinethiolato)(p-tolyl)tin(IV), [Sn(C₅H₄NS)₃(C₇H₇)]. *Acta Crystallogr. C* **1994**, *50*, 206–209. [[CrossRef](#)]
29. Huber, F.; Schmiedgen, R.; Schürmann, M.; Barbieri, R.; Ruisi, G.; Silvestri, A. Mono-organotin(IV) and Tin(IV) Derivatives of 2-Mercaptopyridine and 2-Mercaptopyrimidine: X-ray Structures of Methyl-tris(2-pyridinethiolato)tin(IV) and Phenyl-tris(2-pyridinethiolato)tin(IV)·1.5CHCl₃. *Appl. Organomet. Chem.* **1997**, *11*, 869–888. [[CrossRef](#)]
30. Schürmann, M.; Schmiedgen, R.; Huber, F.; Silvestri, A.; Ruisi, G.; Barbieri Paulsen, A.; Barbieri, R. Mono-aryltin(IV) and mono-benzyltin(IV) complexes with pyridine-2-carboxylic acid and 8-hydroxyquinoline. X-ray structure of p-chloro-phenyl-tris(8-quinolinato)tin(IV)·2CHCl₃. *J. Organomet. Chem.* **1999**, *584*, 103–117. [[CrossRef](#)]
31. Schöne, D.; Gerlach, D.; Wiltzsch, C.; Brendler, E.; Heine, T.; Kroke, E.; Wagler, J. A Distorted Trigonal Antiprismatic Cationic Silicon Complex with Ureato Ligands: Syntheses, Crystal Structures and Solid State ²⁹Si NMR Properties. *Eur. J. Inorg. Chem.* **2010**, *2010*, 461–467. [[CrossRef](#)]
32. Bohme, U. *CSD Private Communication* **2020**, CCDC 2025957.
33. Yang, J.; Verkade, J.G. Non-catalyzed addition reactions of Cl₃SiSiCl₃ with 1,2-diketones, 1,2-quinones and with a 1,4-quinone. *J. Organomet. Chem.* **2002**, *651*, 15–21. [[CrossRef](#)]
34. Feng, Y.-L.; Zhang, F.-X.; Kuang, D.-Z.; Yang, C.-L. Two Novel Dibutyltin Complexes with Trimers and Hexanuclear Based on the Bis(5-Cl/Me-salicylaldehyde) Carbohydrazide: Syntheses, Structures, Fluorescent Properties and Herbicidal Activity. *Chin. J. Struct. Chem.* **2020**, *39*, 682–692. [[CrossRef](#)]

35. Ma, C.; Tian, G.; Zhang, R. New triorganotin(IV) complexes of polyfunctional S,N,O-ligands: Supramolecular structures based on $\pi\cdots\pi$ and/or C–H $\cdots\pi$ interactions. *J. Organomet. Chem.* **2006**, *691*, 2014–2022. [[CrossRef](#)]
36. Boyer, J.; Brelière, C.; Carré, F.; Corriu, R.J.P.; Kpoton, A.; Poirier, M.; Royo, G.; Young, J.C. Five-co-ordinated Silicon Compounds: Geometry of Formation by Intramolecular Co-ordination. Crystal Structure of 2-(Dimethylaminomethyl)phenyl-I-naphthylsilane. *J. Chem. Soc. Dalton. Trans.* **1989**, *1*, 43–51. [[CrossRef](#)]
37. Engelhardt, G.; Radeglia, R.; Jancke, H.; Lippmaa, E.; Mägi, M. Zur Interpretation ^{29}Si -NMR-chemischer Verschiebungen. *Org. Magn. Reson.* **1973**, *5*, 561–566. [[CrossRef](#)]
38. Gericke, R.; Wagler, J. Ruthenium Complexes of Stibino Derivatives of Carboxylic Amides: Synthesis and Characterization of Bidentate Sb,E, Tridentate Sb,E₂, and Tetradentate Sb,E₃ (E = N and O) Ligands and Their Reactivity Toward [RuCl₂(PPh₃)₃]. *Inorg. Chem.* **2020**, *59*, 6359–6375. [[CrossRef](#)]
39. Gericke, R.; Wagler, J. (2-Pyridyloxy)arsines as ligands in transition metal chemistry: A stepwise As(III) → As(II) → As(I) reduction. *Dalton Trans.* **2020**, *49*, 10042–10051. [[CrossRef](#)] [[PubMed](#)]
40. Baus, J.A.; Burschka, C.; Bertermann, R.; Fonseca Guerra, C.; Bickelhaupt, F.M.; Tacke, R. Neutral Six-Coordinate and Cationic Five-Coordinate Silicon(IV) Complexes with Two Bidentate Monoanionic N,S-Pyridine-2-thiolato(–) Ligands. *Inorg. Chem.* **2013**, *52*, 10664–10676. [[CrossRef](#)]
41. Wächtler, E.; Gericke, R.; Kutter, S.; Brendler, E.; Wagler, J. Molecular structures of pyridinethiolato complexes of Sn(II), Sn(IV), Ge(IV), and Si(IV). *Main Group Met. Chem.* **2013**, *36*, 181–191. [[CrossRef](#)]
42. Wahlicht, S.; Brendler, E.; Heine, T.; Zhechkov, L.; Wagler, J. 7-Azaindol-1-yl(organo)silanes and Their PdCl₂ Complexes: Pd-Capped Tetrahedral Silicon Coordination Spheres and Paddlewheels with a Pd-Si Axis. *Organometallics* **2014**, *33*, 2479–2488. [[CrossRef](#)]
43. Autschbach, J.; Sutter, K.; Truflandier, L.A.; Brendler, E.; Wagler, J. Atomic Contributions from Spin-Orbit Coupling to ^{29}Si NMR Chemical Shifts in Metallasilatrane Complexes. *Chem. Eur. J.* **2012**, *18*, 12803–12813. [[CrossRef](#)]
44. Wagler, J.; Brendler, E. Metallasilatranes: Palladium(II) and Platinum(II) as Lone-Pair Donors to Silicon(IV). *Angew. Chem. Int. Ed.* **2010**, *49*, 624–627. [[CrossRef](#)]
45. Gualco, P.; Lin, T.-P.; Sircoglou, M.; Mercy, M.; Ladeira, S.; Bouhadir, G.; Pérez, L.M.; Amgoune, A.; Maron, L.; Gabbai, F.P.; et al. Gold–Silane and Gold–Stannane Complexes: Saturated Molecules as σ -Acceptor Ligands. *Angew. Chem. Int. Ed.* **2009**, *48*, 9892–9895. [[CrossRef](#)] [[PubMed](#)]
46. Kameo, H.; Kawamoto, T.; Bourissou, D.; Sakaki, S.; Nakazawa, H. Evaluation of the σ -Donation from Group 11 Metals (Cu, Ag, Au) to Silane, Germane, and Stannane Based on the Experimental/Theoretical Systematic Approach. *Organometallics* **2015**, *34*, 1440–1448. [[CrossRef](#)]
47. Grobe, J.; Lütke-Brochtrup, K.; Krebs, B.; Läge, M.; Niemeyer, H.-H.; Würthwein, E.-U. Alternativ-Liganden XXXVIII. Neue Versuche zur Synthese von Pd(0)- und Pt(0)-Komplexen des Tripod-Phosphanliganden FSi(CH₂CH₂PMe₂)₃. *Z. Naturforsch.* **2007**, *62b*, 55–65. [[CrossRef](#)]
48. Grobe, J.; Krummen, N.; Wehmschulte, R.; Krebs, B.; Läge, M. Alternativ-Liganden. XXXI Nickelcarbonylkomplexe mit Tripod-Liganden des Typs XM'(OCH₂PMe₂)_n(CH₂CH₂PR₂)_{3-n} (M' = Si, Ge; n = 0–3). *Z. Anorg. Allg. Chem.* **1994**, *620*, 1645–1658. [[CrossRef](#)]
49. Spek, A.L. Single-crystal structure validation with the program PLATON. *J. Appl. Cryst.* **2003**, *36*, 7–13. [[CrossRef](#)]
50. Spek, A.L. Structure validation in chemical crystallography. *Acta Crystallogr. D* **2009**, *65*, 148–155. [[CrossRef](#)] [[PubMed](#)]
51. Spek, A.L. PLATON SQUEEZE: A tool for the calculation of the disordered solvent contribution to the calculated structure factors. *Acta Crystallogr. C* **2015**, *71*, 9–18. [[CrossRef](#)]